Chapter 9
Circulation and Mixing in Steady-State Models: Salt Wedge Estuary

Now that we have laid in the previous chapters the basic estuarine hydrodynamic framework, let us present in the following chapters practical applications of the analytical and numerical studies on the circulation in estuaries and its influence in the distributions of properties concentration.

Among the characteristics to be analytically studied in the field of estuary kinematics and dynamics, there are some which may be approximated using a simple geometry and steady-state conditions, where the estuary can be theoretically treated as a one or two-dimensional system. Natural estuarine channels usually don't have uniform transverse sections that may expand and contract in an irregular manner; however, a common characteristic is that a channel's length is much greater than its width. With the aim of applying the concepts developed in the equations of preceding chapters, steady-state analytical solutions for salt wedge, partially mixed and vertical and laterally well-mixed estuaries will be presented in the present and following chapters. With some approximations, these estuaries may have their circulation and salinity stratification simulated with relatively simple analytical models. Although these solutions will only simulate steady-state conditions, and residual motions and salinity stratifications will be obtained, they are of great practical importance because: (i) their solutions may indicate if the estuary is flushing out or not undesirable substances that are discharged into estuaries; and, (ii) may be used to validate non-steady state numeric solutions.

The general kinematic and dynamic characteristics of estuaries classified as salt wedge (types A or 4) by Pritchard (1955), Hansen and Rattray (1966) were presented in Chap. 3. They were studied in laboratory experiments, combining one and two-dimensional models by several investigators such as Farmer and Morgan (1953), Sanders et al. (1953). The water masses in the upper layers of salt wedge estuaries have very low salinities, and their seaward velocities are much higher than the compensating landward motion below a sharp picnocline; in other words, as stated by Geyer and Farmer (1989), a salt-wedge occurs in an estuary when the river discharge is adequate to maintain a strong gradient between fresh and salt water against the mixing tendency of tide and wind-induced turbulence.

L. Bruner de Miranda et al., *Fundamentals of Estuarine Physical Oceanography*,
Ocean Engineering & Oceanography 8, DOI 10.1007/978-981-10-3041-3_9

Due to the continuous seaward motion in the surface layer, the velocity shear at the picnocline interface between fresh and salt water produces an entrapment of some salt water from the wedge into the upper fresh water layer. In this situation, there is little or no mixing of fresh water into the salt wedge. The salt water volume in the upper layer subsequently increases seaward, and a slow upstream movement of water in the salt wedge occurs to compensate for the upward loss into the fresh water.

The water mass in a characteristic salt-wedge has low stratification, with salinity very close to the one of the coastal water and a sharp halocline is between the transition of the lower (salt-wedge) and upper layers. The circulation continuity is provided by the *entrainment* phenomenon generating slow ascending vertical motions across the picnocline due to oscillating internal waves. This type of estuary is usually dominated by the fresh water discharge, and eddy diffusion may only be important in the surface layer above the halocline. In steady-state conditions and with lateral homogeneity, the dominant terms in the salt-balance equation are the vertical and longitudinal advection, and the diffusive longitudinal term can be disregarded. In the upper layer, the eddy diffusion term may also be taken into account under the influence of strong winds.

In these estuaries, the upper layer above the halocline has its velocity mainly forced by the fresh water discharge. A classical example is the South Pass in the delta of the Mississippi river (Mississippi, USA), which maintains nearly steady-state conditions characteristics over several tidal cycles; it may however, be significantly influenced by tidal motions, causing considerable variation in the vertical structure of salinity and velocity within a tidal cycle (Wright 1970). Another example is the seaward reaches of the Itajai-açu river (Santa Catarina, Brazil), which is forced by micro-tides and has been classified as a salt wedge estuary in conditions where river discharges around 300 $m^3\ s^{-1}$, and the saline wedge is displaced landward up to 18 km from its mouth. However, when the river discharge reaches values up to 1000 $m^3\ s^{-1}$, the seawater is completely evacuated through its mouth (Döbereiner 1985, quoted in Schettini (2002)). The salt-wedge extension in the estuarine plume was empirically correlated with the river discharge, presenting an exponential decay with the increase in river discharge (Schettini and Truccolo 1999).

Under the assumption of nearly steady-state conditions, the landward salt-wedge propagation varies mainly at a seasonal time scale, forced by the river discharge. The theory which will be developed in this chapter can't be generalized for all salt wedge estuaries, and holds only for an *arrested* salt wedge estuaries. According to classical authors Farmer and Morgan (1953), Schijf and Schonfeld (1963) (quoted in Geyer and Farmer (1989)); the designation *arrested salt-wedge* for this estuary type refers to a regime in which the pressure gradient force is balanced by inertial and frictional forces within the estuary, and its interfacial structure attains a quasi-steady-state configuration.

In the literature we find studies of salt wedge estuaries forced by meso-tides, for example, the Fraser river estuary (Vancouver, Canada). In this river, the salt-wedge varies along the estuary during the tidal cycle towards an equilibrium condition

against the free surface slope variations. The advancing of the salt-wedge front position vs. time, provided by tracking with echo-sounding images for three sets of observations, indicated that the advance of salt-wedge intrusion length varied from 9 to 18 km for high and low river discharge, respectively (Geyer 1986). The interaction of the tidal flow with the density-driven motion of the salt-wedge, during different phases of the tide and river discharge has been clearly illustrated by Geyer and Farmer (1989), showing that the highly stratified vertical salinity structure, existing at high and low tides, becomes poorly stratified at the end of the flood tide, and the salt-wedge water remains under the strong picnocline at the estuary mouth.

In salt wedge estuaries, which will be analytically investigated in this chapter, the physical process of momentum exchanges in the fresh-salt water interface will be simulated by a shear named *interfacial stress*. This stress, which is force per unit of area, is mainly provided by the river input, and causes a seaward ascending inclination of the salt-wedge (Fig. 9.1). In this figure, we may observe that the longitudinal salinity gradients in the layers above and below the halocline are absent or very low, and in the theoretical treatment of the salt-wedge its dynamical consequences will be disregarded. This figure also indicates the displacement of the salt wedge front position due to the influence of the river discharge variation.

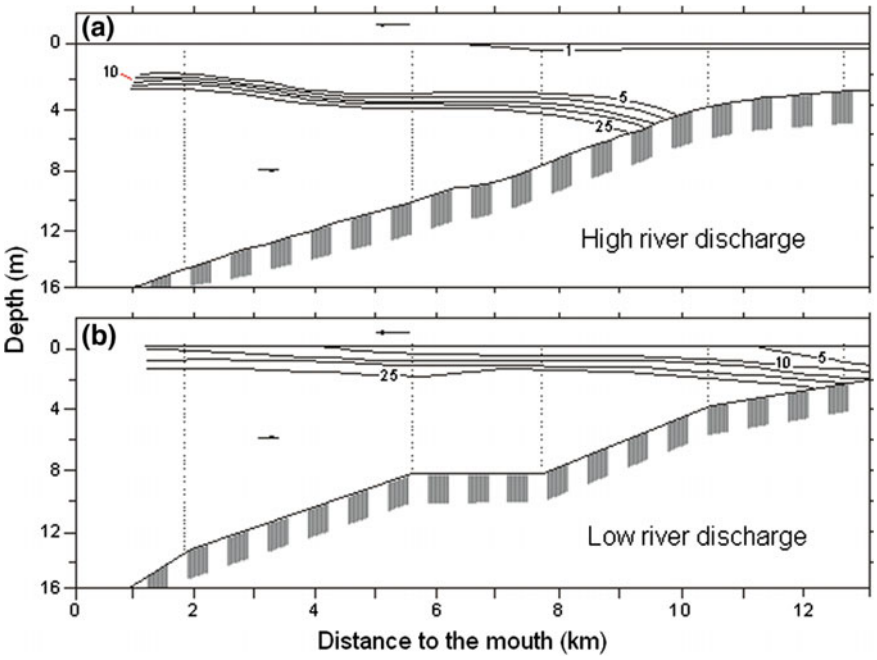

Fig. 9.1 Salinity stratification in a salt wedge estuary in conditions of high (**a**) and low (**b**) river discharge in the river Duwamish (Seattle, USA) (according to Dawson and Tilley 1972)

9.1 Hypothesis and Theoretical Formulation

A salt wedge estuary is schematically represented in Fig. 9.2, with the referential system and the adopted notation of properties and variables in the upper and lower layers indicated with indices 1 and 2, respectively. In this development, the estuary is assumed to be narrow and laterally homogeneous, and the Oz will be oriented in the gravity acceleration direction, which requires a signal change in the mathematical expression of the longitudinal component of the barotropic gradient pressure force (Eq. 8.18a,b, Chap. 8), as its previous orientation was against the gravity acceleration. It should be observed that $\partial\eta/\partial x$ is negative and the interface slopes in the landward direction.

Taking into account the Oxz axis orientation, the gradient pressure force has the following expression:

$$-\frac{1}{\rho}\left(\frac{\partial p}{\partial x}\right) = g\left(\frac{\partial \eta}{\partial x}\right) - \frac{g}{\rho}\left(\int_{z}^{\eta} \frac{\partial \rho}{\partial x} dz\right). \tag{9.1}$$

The first theoretical investigations to calculate the vertical velocity profile and the salt intrusion length of the salt wedge estuary, using the continuity and motion equations in the upper and lower layers, were developed by Farmer and Morgan (1953), Sanders et al. (1953), followed by Shi-Igai and Sawamoto (1969). In these studies, the main results of which are described in this chapter, the motion attains a

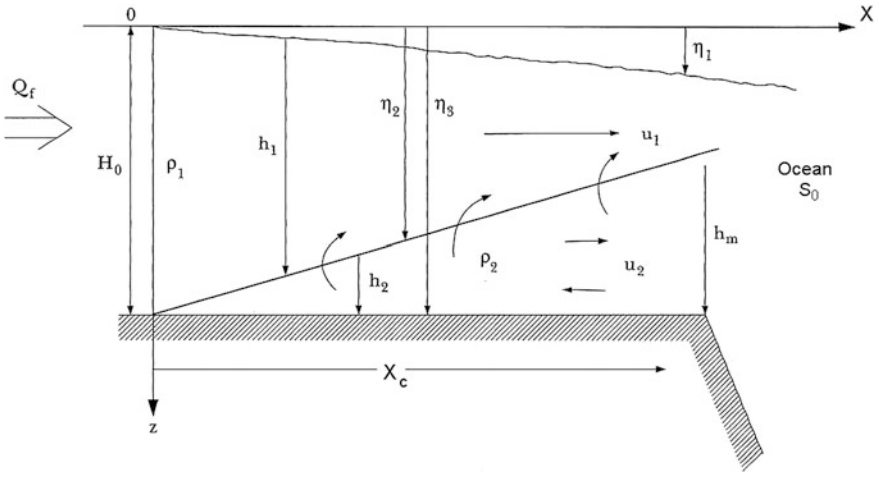

Fig. 9.2 Schematic diagram of a salt wedge estuary. Variables and properties used in the theoretical development for the upper and lower layers are indicated by indices 1 and 2, respectively. $\eta_{1,2}$, $u_{1,2}$, $h_{1,2}$ are the slopes of the free surface and the interface in relation to the surface level, the velocities, and the layers thicknesses, respectively (adapted from Farmer and Morgan 1953). X_c is the salt-wedge intrusion length and h_m is its height at the estuary mouth

quasi-steady condition, in which the baroclinic pressure gradient is balanced by inertial and frictional forces within the estuary. In these two-layer motions, the following simplifying hypotheses were adopted:

- Simple geometry: width (B) and depth (H_0) constants;
- No vertical mixing between the upper and lower layers;
- The u-velocity component in the upper layer is generated by the river discharge;
- The wind stress on the surface is disregarded;
- The interfacial shear stress $f_i[f_i] = [ML^{-1}T^{-2}]$, on the halocline is proportional to the square of the upper layer velocity, and the proportionality constant, k, which is non-dimensional,

$$f_i = k\rho_1 u_1^2, \tag{9.2}$$

- The velocity in the salt wedge, u_2, is much less than in the upper layer, $u_2 << u_1$;
- The longitudinal acceleration due to the advection, $u_2 \frac{\partial u_2}{\partial x}$, and the volume transport in the salt-wedge, $Q_2, [Q_2] = [L^3T^{-1}]$ will be disregarded ($Q_2 \ll Q_f$).

The comparison of the interfacial shear stress f_i (Eq. 9.2) with the bottom shear stress (τ_{Bx}) of a one-dimensional estuarine channel (Eq. 8.31, Chap. 8) indicates that the coefficient, k, corresponds to the ratio of the gravity acceleration to the square of the Chézy coefficient (g/C_y^2).

The theoretical development of this analytical model has the following objectives: (i) Calculate the vertical velocity profile u = u(x, z), the free surface and the halocline interface slopes $d\eta_1(x)/dx$ and $d\eta_2(x)/dx$, respectively (ii) Determination of the salt-wedge intrusion length, X_C, (Fig. 9.2) and the energy dissipation due to the interfacial shear stress and viscosity. To achieve this, the hydrodynamics formulation must take into account the mass and momentum conservation equations, which must be adequately simplified and solved in order to satisfy the specified boundary and integral boundary conditions.

9.2 Circulation and Salt-Wedge Intrusion

9.2.1 The Upper Layer

The one-dimensional equations of motion and the continuity (Eqs. 8.67 and 8.68, Chap. 8) are used to formulate the hydrodynamics of the upper layer which, according to the simplifying conditions, are:

$$\frac{\partial(uuA)}{\partial x} = -\frac{A}{\rho}\frac{\partial p}{\partial x} - \frac{1}{\rho}\tau_{Bx}P_m, \tag{9.3}$$

and

$$\frac{\partial(uA)}{\partial x} = 0. \tag{9.4}$$

The simplified equation of the state of seawater (Eq. 8.71, Chap. 8) will provide the hydrodynamic closure of this equation system,

$$\rho(S) = \rho_0(1 + \beta S). \tag{9.5}$$

The salinity in the upper, $S_1 \approx 0$, and lower layers, $S_2 = S_0$, will be taken as constants, and the salinity at the coastal region, S_0, is the only salt source for the estuarine water mass formation; from the equation of state of seawater Eq. (9.5), it follows that the density in these layers are constants and $\rho_1 < \rho_2$.

For the layer above the halocline, the last term on the right-hand-side of Eq. (9.3), representing the formulation of the bottom energy dissipation, will as a first approximation be substituted by the interfacial shear stress (Eq. 9.2). As the estuary width (B) is usually much greater than its depth $(B \gg H_0)$, the wet perimeter, P_m, in Eq. (9.3) may be approximated by its width ($P_m = B$). As in Eqs. (9.3) and (9.4), the partial derivation may be changed to the total derivation, because x is only independent variable in these equations, and they may be rewritten as:

$$\frac{d(uuA)}{dx} = gA\frac{\partial \eta}{\partial x} - Bku^2, \tag{9.6}$$

and

$$\frac{d(uA)}{dx} = 0. \tag{9.7}$$

Under the assumption that k is a known coefficient, this equation system is closed and the two unknowns, $u = u(x)$ and $\eta = \eta(x)$, may be calculated.

Applying these equations to the upper layer (1) where $\eta_1(x) \leq z \leq \eta_2(x)$ and $h_1(x) = \eta_2(x) - \eta_1(x)$, and taking into account the particular geometry of the problem, the continuity equation is simplified to:

$$\frac{d[Bu_1(x)h_1(x)]}{dx} = 0. \tag{9.8}$$

In this equation, $h_1(x)$ is the thickness of the upper layer, and it is possible to calculate the uniform velocity field, $u_1 = u_1(x)$, integrating from the estuary head ($x = 0$) seaward up to a generic position x,

$$Bu_1(x)h_1(x) - Q_f = 0, \tag{9.9}$$

and

$$u_1(x) = \frac{Q_f}{Bh_1(x)}. \tag{9.10}$$

This last result indicates that if the halocline or picnocline depth $h_1(x)$ is known, the cross sectional mean velocity, $u_1 = u_1(x)$, in the upper layer may be calculated.

As B = const. Equation (9.8) may be rewritten as

$$\frac{d[u_1(x)h_1(x)]}{dx} = \frac{dQ_1(x)}{dx} = 0, \tag{9.11}$$

and the product of the mean velocity in the upper layer by the halocline depth, $Q_1(x)$, with dimension $[Q_1] = [L^2T^{-1}]$, is independent of the longitudinal distance (x), and this value is equal to Q_f/B, or

$$u_1(x)h_1(x) = \frac{Q_f}{B}; \text{or } u_1(x) = \frac{Q_f}{Bh_1(x)}. \tag{9.12}$$

With this procedure applied to the salt-wedge, it follows the trivial result due to the hypothesis that the volume transport in the lower layer is zero

$$Bu_2(x)h_2(x) = Q_2 = 0, \tag{9.13}$$

where $h_2(x)$ is the lower layer thickness. This result indicates that the mean depth velocity, $\bar{u}_2(x)$, is equal to zero. However, the salt-wedge presents a vertical velocity gradient (vertical shear), whose profile $u_2 = u_2(z)$ will be determined during this theoretical development.

Now, let us continue, applying the equation of motion (9.6) to the upper layer:

$$\frac{d[u_1(x)u_1(x)Bh_1(x)]}{dx} = gBh_1(x)\frac{d\eta_1(x)}{dx} - kBu_1^2(x). \tag{9.14}$$

Calculating the derivative of the first term of this equation, it follows that:

$$u_1(x)\frac{d[u_1(x)h_1(x)]}{dx} + u_1(x)h_1(x)\frac{du_1(x)}{dx} = gh_1(x)\frac{d\eta_1(x)}{dx} - ku_1^2(x), \tag{9.15}$$

and combining with Eq. (9.11), gives

$$u_1(x)h_1(x)\frac{du_1(x)}{dx} = gh_1(x)\frac{d\eta_1(x)}{dx} - ku_1^2(x). \tag{9.16}$$

The only unknown in this equation is the slope of the free surface $\eta_1 = \eta_1(x)$, because the velocity $u_1 = u_1(x)$ has already been determined by the Eq. (9.10). Hence, the unknown $\eta_1 = \eta_1(x)$ may be calculated by the following expression:

$$\eta_1(x) = \frac{k}{g}\int_0^x \frac{u_1^2(x)}{h_1(x)}dx + \frac{1}{2g}[u_1^2(x) - u_1^2(0)], \tag{9.17}$$

or, taking into account the $u_1(x)$ solution (Eq. 9.10), where $u_1(0) = Q_f/BH_0 = u_f$, the solution may also be expressed as:

$$\eta_1(x) = \frac{kQ_f^2}{gB^2}\int_0^x \frac{1}{h_1^3(x)}dx + \frac{1}{2g}[u_1^2(x) - u_f^2]. \tag{9.18}$$

As with Eqs. (9.10) and (9.18), it is possible to calculate $u_1(x)$ and $\eta_1(x)$, and thus the hydrodynamic problem for the upper layer of the salt wedge estuary is solved.

In the following development, let us calculate the relationship between the first derivatives of the free surface slope $(d\eta_1/dx)$ and that of the salt-wedge $(d\eta_2/dx)$, which will be used later to calculate the salt-wedge intrusion length. Thus, the first term of Eq. (9.16) may be combined with Eq. (9.10), resulting in:

$$u_1(x)h_1(x)\frac{d[u_1(x)]}{dx} = u_1(x)h_1(x)\frac{d}{dx}\left[\frac{Q_f}{Bh_1(x)}\right] = -\frac{[u_1(x)Q_f]}{Bh(x)_1}\frac{d[(h_1(x)]}{dx}, \tag{9.19}$$

or

$$-\frac{u_1(x)Q_f}{Bh_1(x)}\left[\frac{d\eta_2(x)}{dx} - \frac{d\eta_1(x)}{dx}\right] = -u_1^2(x)\left[\frac{d\eta_2(x)}{dx} - \frac{d\eta_1(x)}{dx}\right]. \tag{9.20}$$

Combining Eqs. (9.20) and (9.16) and rearranging its terms, it follows that:

$$\left[\frac{gh_1(x)}{u_1^2(x)} - 1\right]\left[\frac{d\eta_1(x)}{dx} - \frac{d\eta_2(x)}{dx}\right] = k. \tag{9.21}$$

Taking into account that

$$\left[\frac{gh_1(x)}{u_1^2(x)}\right] \gg 1, \tag{9.22}$$

Equation (9.21) is reduced to the following relationship between the first derivatives of the sea surface slope $\eta_1(x)$ and $\eta_2(x)$:

$$\frac{gh_1(x)}{u_1^2(x)}\left[\frac{d\eta_1(x)}{dx}\right]+\frac{d\eta_2(x)}{dx}=k. \tag{9.23}$$

With Eq. (9.10), it is possible to calculate the volume transport per unit width of the cross-section (Q_1),

$$\frac{Q_f}{B}=Q_1, \tag{9.24}$$

which is independent of the longitudinal distance x (Eq. 9.11). Its introduction into the Eq. (9.23) is convenient, and to achieve this, it is necessary to multiply and divide the factor $d\eta_1(x)/dx$ by the square of the depth of the upper layer, $h_1^2(x)$. Then, according to Officer (1976) the result is:

$$\frac{gh_1^3(x)}{Q_1^2}\left(\frac{d\eta_1(x)}{dx}\right)+\frac{d\eta_2(x)}{dx}=k. \tag{9.25}$$

All terms on the left-hand-side of this equation are dimensionless.

9.2.2 The Lower Layer (Salt-Wedge)

According to the simplified physics adopted for this estuary, in the salt-wedge ($\eta_2 \le z \le \eta_1$) which has a thickness equal to $h_2(x)$, the velocity u_2 is much less than that of the upper layer ($u_2 \ll u_1$), and the advective acceleration may be disregarded. This layer characteristic has already been demonstrated in the model that used only the continuity and salt conservation equations (Eqs. 7.43 and 7.44), resulting in constant values of the longitudinal velocity component in the upper layer of the salt wedge estuary, and $u_1 > u_2$ (Fig. 7.3, Chap. 7). However, the motion direction in the halocline is reverted due to the entrainment and the bottom friction, and it is expected that this velocity component, although with low intensity, should present a vertical shear ($\partial u_2/\partial z \neq 0$). Thus, at any given longitudinal distance this velocity (u_2) is dependent on the depth. According to the longitudinal velocity component of the bi-dimensional equation of motion (equation, 8.57a, Chap. 8), the hydrodynamic equilibrium is reduced to the balance of the barotropic pressure gradient generated by the interface slopes η_1 and η_2 and the frictional force,

$$\frac{1}{\rho_2}\frac{\partial p_2}{\partial x}=\frac{\partial}{\partial z}\left[N_z\frac{\partial u_2(x,z)}{\partial z}\right], \tag{9.26}$$

This equation is a simplified formulation of the bi-dimensional equation of motion in the Oxz plane, whose gradient pressure force only has the barotropic

component, because the density (ρ_2) at this layer is independent of the longitudinal distance. According to the linear equation of state (Eq. 9.5), knowing the salinity, the value of which may be obtained from experimental results, the density in the lower layer (ρ_2) is also known. Under the assumption that the kinematic eddy viscosity coefficient (N_z) is given, the only unknown in the Eq. (9.26) is the velocity in the salt-wedge, $u_2 = u_2(x, z)$, which may be calculate as follows.

The pressure p_2 at a depth z of the salt-wedge (Fig. 9.2) may be calculated by:

$$p_2(x,z) = g\rho_1(\eta_2 - \eta_1) + g\rho_2(z - \eta_2). \tag{9.27}$$

By derivation of this equation in relation to the longitudinal distance (x), it follows that the expression for the barotropic pressure gradient is:

$$\frac{\partial p_2}{\partial x} = -g\rho_1[\frac{\partial \eta_1(x)}{dx}] - g(\rho_2 - \rho_1)[\frac{d\eta_2(x)}{dx}], \tag{9.28}$$

which is independent of the depth and is dependent only on the slopes of the free surface and the salt-wedge.

Proceeding with the integration of Eq. (9.26) in the vertical direction of the salt-wedge, and taking into account that the first term is the barotropic pressure gradient yields,

$$\frac{\partial p_2}{\partial x}[\eta_3(x) - \eta_2(x)] = \rho_2 N_z[\frac{\partial u_2(x,\, z)}{\partial z}|_{z=\eta_3} - \frac{\partial u_2(x,\, z)}{\partial z}|_{z=\eta_2}]. \tag{9.29}$$

Remembering that $h_2(x) = \eta_3(x) - \eta_2(x)$ is the salt-wedge thickness, as indicated Fig. 9.2, and the two terms of its right member are the components of the shear stress acting at the bottom ($z = \eta_3$) and surface ($z = \eta_2$) of the salt wedge, this equation may be rewritten as:

$$h_2(x)\frac{\partial p_2}{\partial x} = \tau_{zx}|_{z=\eta_3} - \tau_{zx}|_{z=\eta_2}. \tag{9.30}$$

Combining this equation with Eq. (9.28) we have

$$-gh_2(x)[\rho_1 \frac{d\eta_1(x)}{dx} + (\rho_2 - \rho_1)\frac{d\eta_2(x)}{dx}] = \tau_{zx}|_{z=\eta_3} - \tau_{zx}|_{z=\eta_2}. \tag{9.31}$$

In this equation, the shear stress on the superior interface of the salt-wedge is, by hypothesis, equal to the interfacial stress ($f_i = k\rho_1 u_1^2$). Then,

$$\tau_{zx}|_{z=\eta_3} = \tau_{zx}(\eta_2) = f_i = k\rho_1 u_1^2(x), \tag{9.32}$$

and the Eq. (9.31) may be rewritten as

$$-gh_2(x)[\rho_1 \frac{d\eta_1(x)}{dx} + (\rho_2 - \rho_1)\frac{d\eta_2(x)}{dx}] = \tau_{zx}|_{z=\eta_3} - k\rho_1 u_1^2(x). \tag{9.33}$$

As the term on the left-hand side of Eq. (9.26) is the barotropic pressure gradient, the velocity may be approximated by the following quadratic expression (Officer 1976): $u_2(x,z) = a + bz + cz^2$. The coefficients of this expression may be determined by applying the boundary and integral boundary conditions, and one of these coefficients will be function of x. In this development, the Oz axis will have its origin at the bottom and will be oriented upward, against the gravity acceleration. The new ordinate will be denoted by $(\overline{z})$; it will be related to the orientation of the first vertical variable (z) orientation by the relation $\overline{z} = H_0 - z$, and at the bottom $z = H_0$ and $\overline{z} = 0$. With the introduction of this new variable, the vertical velocity profile in the salt-wedge will be given by

$$u_2(x, \overline{z}) = a + b\overline{z} + c(\overline{z})^2, \tag{9.34}$$

and the coefficients a, b and c may be calculated with the following boundary and integral boundary conditions:

$$u_2(x, \overline{z})|_{\overline{z}=0} = 0, \tag{9.35}$$

$$u_2(x, \overline{z})|_{\overline{z}=h_2} = u_1(x), \tag{9.36}$$

and

$$\int_0^{h_2} u_2(x, \overline{z})d\overline{z} = Q_2 = 0. \tag{9.37}$$

The latter condition is due to the hypothesis that the net volume transport in the salt-wedge is zero.

Applying the boundary condition (9.35), it follows immediately that a = 0, and for the remaining conditions, (9.36) and (9.37), the result is an algebraic system of two equations and two unknowns b and c,

$$u_1 = bh_2 + ch_2^2, \tag{9.38}$$

and

$$\frac{1}{2}bh_2^2 + \frac{1}{3}ch_2^3 = 0. \tag{9.39}$$

This system of equations may be solved, giving the results: $b = -2u_1/h_2$ and $c = 3u_1/h_2^2$, and the vertical velocity profile $u_2 = u_2(x, z)$ has the following expression:

$$u_2(x, \overline{z}) = -\frac{2u_1}{h_2}\overline{z} + \frac{3u_1}{h_2^2}\overline{z}^2, \tag{9.40}$$

or, returning to the z variable

$$u_2(x, z) = -\frac{2u_1}{h_2}(H_0 - z) + \frac{3u_1}{h_2^2}(H_0 - z)^2. \tag{9.41}$$

Analysis of these solutions indicates that the velocity is zero at $\overline{z} = (2/3)h_2$ and $z = H_0$ - $(2/3)h_2$, and there is a minimum point in this vertical velocity profile at depth $\overline{z} = (1/3)h_2$ or $z = H_0 - (1/3)h_2$. At this depth, the minimum velocity at the salt-wedge is $u_2 = -(1/3)u_f$.

9.2.3 Vertical Velocity Profile

The combined solutions of Eqs. (9.10) and (9.41), used to calculate the velocities $u_1 = u_1(x)$ and $u_2 = u_2(x,z)$ in the upper and lower layers of the halocline, respectively, are the theoretical solutions of the vertical velocity profile in the salt wedge estuary, which are driven by the fresh water discharge and the barotropic influences of the free surface slope and salt-wedge interface with the river discharge, respectively. The energy dissipating forces, which counteract the river discharge and baroclinic pressure gradient, are the vertical friction, due to the viscosity, and the interfacial and bottom shear stresses.

According to classical investigations cited in the article of Geyer and Farmer (1989), the designation *arrested salt wedge* for this estuary refers to a regime in which the baroclinic pressure gradient is balanced by inertial and frictional forces within the estuary, and its interfacial structure attains a quasi-steady configuration. A practical example of this theory will be presented at the end of this chapter.

9.2.4 Salt-Wedge Intrusion Length

Knowing the analytical expression of the vertical velocity profile in the salt wedge estuary (Eqs. 9.40 or 9.41), it is possible to calculate the frictional stresses, $(\tau_{zx}|_{z=\eta_3})$ and $(\tau_{zx}|_{z=\eta_2})$ at the depths $z = H_0$ (or $\overline{z} = 0$) and $z = \eta_2$ (or $\overline{z} = h_2$), respectively,

$$\tau_{zx}|_{z=\eta_3} = \tau_{zx}(\eta_3) = -\rho_2 N_z \frac{\partial u_2}{\partial \overline{z}}|_{\overline{z}=0} = \frac{2\rho_2 N_z u_1}{h_2}, \tag{9.42}$$

and

$$\tau_{zx}|_{z=\eta_2} = \tau_{zx}(\eta_2) = -\rho_2 N_z \frac{\partial u_2}{\partial \overline{z}}|_{\overline{z}=h_2} = -\frac{4\rho_2 N_z u_1}{h_2}. \tag{9.43}$$

Combining these equations and taking into account that the first term on the right-hand-side of Eq. (9.43) is the interfacial frictional shear that may be approximated by Eq. 9.32, it follows that,

$$\tau_{zx}|_{\overline{z}=0} = -\frac{1}{2}\tau_{zx}|_{\overline{z}=h_2} = \frac{1}{2} f_i = \frac{1}{2}\rho_1 k u_1^2. \tag{9.44}$$

By subtracting Eqs. (9.42) and (9.43),

$$\tau_{zx}|_{z=\eta_3} - \tau_{zx}|_{z=\eta_2} = \frac{6\rho_2 N_z u_1}{h_2}. \tag{9.45}$$

In this equation, the quantity $\tau_{zx}|_{z=\eta_2} = \tau_{zx}(\eta_2)$ is equal to the interfacial shear stress (f_i), and the following relationship exists between the coefficients k and the kinematic eddy viscosity coefficient, N_z,

$$N_z = k\left(\frac{\rho_1 h_2 u_1}{4\rho_2}\right), \tag{9.46}$$

and substituting this result into Eq. (9.45),

$$\tau_{zx}|_{z=\eta_3} - \tau_{zx}|_{z=\eta_2} = \frac{3}{2} k\rho_1 u_1^2. \tag{9.47}$$

Finally, combining this result with Eq. (9.31) gives the following relationship of the derivatives of sea surface ($d\eta_1/dx$) and salt-wedge ($d\eta_2/dx$), slopes:

$$-gh_2\left[\rho_1 \frac{d\eta_1(x)}{dx} + (\rho_2 - \rho_1)\frac{d\eta_2(x)}{dx}\right] = \frac{3}{2}\rho_1 k u_1^2. \tag{9.48}$$

As an artifice, multiplying the term on the left-hand-side by the ratio h_1^2/h_1^2 and dividing both equation members by $\rho_1 u_1^2$ and using the approximation $\rho_1 \approx \rho_2$, yields

$$-\frac{gh_1^2 h_2}{Q_1^2}\left[\frac{d\eta_1(x)}{dx} + \delta\frac{d\eta_2(x)}{dx}\right] = \frac{3}{2}k, \tag{9.49}$$

where $(u_1 h_1)^2 = Q_1^2$ is the square value of the river discharge per unit width, and the quantity δ is defined by

$$\delta = \frac{\rho_2 - \rho_1}{\rho_2} = \frac{\Delta\rho}{\rho_2}. \tag{9.50}$$

Equations (9.25) and (9.49) are components of an algebraic system with two unknowns, $d\eta_1(x)/dx$ and $d\eta_2(x)/dx$. Then, for the second unknown the result is;

$$\frac{d\eta_2(x)}{dx}\left[\frac{h_2(x)}{h_1(x)} - \frac{g h_1^2(x)\delta h_2(x)}{Q_1^2}\right] = k\left[\frac{h_2(x)}{h_1(x)} + \frac{3}{2}\right]. \tag{9.51}$$

A trivial solution of this equation is to consider that the interfacial shear stress ($f_i = k\rho_1 u_1^2$) is equal to zero, which may be simulated with k = 0. However, for a salt-wedge occurrence ($k \neq 0$) the Eq. (9.51) may be solved for $d\eta_2/dx$ and integrated to calculate the unknown, $\eta_2 = \eta_2(x)$,

$$\eta_2(x) = \int_0^x \left\{\frac{k\left[\frac{h_2(x)}{h_1(x)} + \frac{3}{2}\right]}{\left[\frac{h_2(x)}{h_1(x)} - \frac{g' h_1^2(x) h_2(x)}{Q_1^2}\right]}\right\} dx. \tag{9.52}$$

As the main objective of this topic is to calculate the salt-wedge intrusion length, X_c, Eq. (9.51) will be used for this purpose. As the ordinate η_3 may be taken as a constant, let us apply the approximation,

$$\frac{d[h_2(x)]}{dx} = -\frac{d[\eta_2(x)]}{dx}, \tag{9.53}$$

and combining this with Eq. (9.51), factoring in the first term by the ratio h_2/h_1, and rearranging the terms, we have,

$$h_2(x)\left[1 - \frac{g' h_1^3(x)}{Q_1^2}\right]\frac{dh_2(x)}{dx} = -k\left[h_2(x) + \frac{3h_1(x)}{2}\right], \tag{9.54}$$

and analysis of the salt wedge estuary (Fig. 9.2) showed the following relationships:

$$H_0 = h_1 + h_2 + \eta_1 \text{ and } h_1 + h_2 \gg \eta_1. \tag{9.55}$$

Thus, Eq. (9.54) may be rewritten as a function of the non-dimensional salt-wedge height $H(x) = h_2(x)/H_0$, which varies in the interval $0 \leq H(x) < 1$, and the differential $dh_2(x)$ is

$$dh_2(x) = H_0 dH(x), \tag{9.56}$$

and combined with the relationship (9.55) the initial solution is:

$$H(x)[1-\frac{g'H_0^3[1-H(x)]^3}{Q_1^2}]\frac{dH(x)}{dx}=-\frac{k[3-H(x)]}{2H_0}. \tag{9.57}$$

Considering the ratio

$$(\frac{Q_1^2}{g'H_0^3})=\gamma, \tag{9.58}$$

which may be considered constant, because in the hypothesis of a steady-state condition the fresh water (Q_f) is also constant, Eq. (9.57) can be rewritten as,

$$H(x)\{\ \frac{[1-H(x)]^3-\gamma}{\gamma}\}\ \frac{dH(x)}{dx}=k\frac{[3-H(x)]}{2H_0}. \tag{9.59}$$

This equation is an ordinary differential equation with separable variables which may be integrated from the landward limit of the salt-wedge, x = 0, up to a seaward longitudinal position, x,

$$(\frac{k\gamma}{2H_0})x=\int_0^H\frac{H(x)[1-H(x)]^3-\gamma H(x)}{[3-H(x)]}dH. \tag{9.60}$$

As a case limit for this result, we may observe that for $x \to 0$, implies that $H(x) \to 0$, because by definition $H(x) = h_2(x)/H_0$, and $h_2(0) = 0$ at the interior limit of the salt-wedge (Fig. 9.2).

Developing the algebraic expression of the integrand in Eq. (9.60), and using the additive propriety of integrals yields:

$$\begin{aligned}(\frac{k\gamma}{2H_0})x=(1-\gamma)&\int_0^H\{\ \frac{H(x)}{[3-H(x)]}\}\ dH\\&-3\int_0^H\{\ \frac{H^2(x)}{[3-H(x)]}\}dH+3\int_0^H\{\ \frac{H^3(x))}{[3-H(x)]}\}\ dH\\&-\int_0^H\{\ \frac{H^4(x)}{[3-H(x)]}\}\ dH.\end{aligned} \tag{9.61}$$

Taking into account the following algebraic equalities:

$$\frac{H^2(x)}{[3-H(x)]}=-H(x)+3\frac{H(x)}{[3-H(x)]}, \tag{9.62}$$

$$\frac{H^3(x)}{[3-H(x)]} = -H^2(x) - 3H(x) + 9\frac{H(x)}{[3-H(x)]}, \tag{9.63}$$

and

$$\frac{H^4(x)}{[3-H(x)]} = -H^3(x) - 3H^2(x) - 9H(x) + 27\frac{H(x)}{[3-H(x)]}. \tag{9.64}$$

Substituting them into the integrands of the lasts three terms of the right-hand-side of expression (9.61) and simplifying the result, we have:

$$\frac{k\gamma}{2H_0}x = -(\gamma-8)\int_0^H \{\ \frac{H(x)}{[3-H(x)]}\}\ dH + 3\int_0^H H(x)dH + \int_0^H H^3(x)dH. \tag{9.65}$$

The first term of the right-hand-side of this equation may be easily integrate remembering that its indefinite integral is given by (Granville et al. 1956),

$$\int \frac{H}{(3-H)}dH = 3 - H - 3\ln(3-H). \tag{9.66}$$

The integration of the second and third terms is immediate, and follow the relationship between the longitudinal distance, x, and the non-dimensional salt-wedge height:

$$\frac{k\gamma}{2H_0}x = \frac{3}{2}H^2(x) + \frac{1}{4}H^4(x) + (\gamma+8)\{\ 3\ln[\frac{3-H(x)}{3}] + H(x)\}\ . \tag{9.67}$$

Equation (9.58), which defines the quantity γ, is a function of the river discharge, mass stratification and the estuary depth. As $Q_1 = u_1(0)H_0 = u_fH_0$ at the estuary head, γ may be expressed as:

$$\gamma = \frac{u_f^2}{g'H_0} = \frac{u_f^2}{g\frac{\Delta\rho}{\rho_2}H_0}. \tag{9.68}$$

This dimensionless number is equal to the square of the densimetric Froude number ($\gamma = F_m$), defined in the Chap. 2 (Eq. 2.39). This number has been investigated by Farmer and Morgan (1953), who simulated the circulation in salt wedge estuaries and observed that this number converges to 1 ($F_m \rightarrow 1$) in the transition of the fresh water flow to the salt water reservoir. In the salt wedge estuary, this number may be estimated using the following data: $g = 10\ ms^{-2}$, $u_f = 0.1\ ms^{-1}$, $\Delta\rho/\rho_2 = 3.0 \times 10^{-4}$ and $H_0 = 10$ m, resulting in $\gamma = 0.3$. As $g < 1 \rightarrow F_m < 1$, this indicates a subcritical vertical stratification which is

characteristic of highly stratified estuaries. Usually the parameter $\gamma \ll 8$ and may be disregarded in the last term of Eq. (9.67), which may be simplified for praticality to:

$$\frac{k\gamma}{2H_0}x = \frac{3}{2}H^2(x) + \frac{1}{4}H^4(x) + 8\{\ 3\ln[\frac{3 - H(x)}{3}] + H(x)\}\ . \tag{9.69}$$

To calculate the salt-wedge intrusion length (X_c), let us define its non-dimensional depth at the estuary mouth as $H_m = h_m/H_0$ (Fig. 9.2), which can be obtained with observational data. Then, if the depth $H \rightarrow H_m$ in the second member of Eq. (9.69), the generic distance x of the first member approaches X_c, and this may be calculated by:

$$\frac{k\gamma}{2H_0}X_c = \frac{3}{2}H_m^2 + \frac{1}{4}H_m^4 + 8\{\ 3\ln[\frac{3 - H_m}{3}] + H_m\}\ . \tag{9.70}$$

Solving this equation for the salt-wedge intrusion length, X_c, it follows that:

$$X_c = 2\frac{g'H_0^2}{ku_f^2}[\frac{3}{2}H_m^2 + \frac{1}{4}H_m^4 + 8\{\ 3\ln[\frac{(3 - H_m)}{3}] + H_m\}\ . \tag{9.71}$$

This result indicates that X_c is directly proportional to the square of the estuary depth (H_0^2), and inversely proportional to the coefficient of interfacial frictional shear (k) and the square of the velocity generated by the river discharge (u_f). Besides the seasonal variation of u_f, its input in the estuary may be the altered by utilization of river water in agriculture, industrial and for domestic use, interfering with the salt-wedge intrusion length. The estuarine channel depth (H_0) may decrease due to sedimentation processes and may be modified by dredging. Consequently, the theoretical results (Eq. 9.71) clearly indicate that human interference may have anomalous influences on this natural environment.

The salt-wedge configuration can be conveniently analysed through its non-dimensional formulation, which may be obtained by the ratio of Eqs. (9.69) and (9.70),

$$\frac{x}{X_c} = [\frac{H^2(x)}{H_m}].\{\ \frac{\frac{3}{2} + \frac{H^2(x)}{4} + \frac{8}{H^2(x)}[3\ln(\frac{3-H(x)}{3}) + H(x)]}{\frac{3}{2} + \frac{H_m^2}{4} + \frac{8}{H_m^2}[3\ln(\frac{3-H_m}{3}) + H_m]}\ \}\ . \tag{9.72}$$

From this solution, we have the following limiting cases:

- When $H = H_m \rightarrow x/X_c = 1$; and
- For $H = 0 \rightarrow x/X_c = 0$.

These results are equivalent to the simplest analytical expressions obtained by Farmer and Morgan (1953); Officer (1976) for determination of the steady-state

configuration of the salt-wedge. Analysis of Eq. (9.72) indicates that there will be similarities in the salt wedge configurations for different estuaries. These similarities are due to the fact that when the interfacial Froude number is less than one, the salt-wedge configuration is independent of the water mass salinity in the coastal sea and of the velocity generated by the river discharge. The non-dimensional salt-wedge configuration deduced by Farmer & Morgan (op. cit), with the notation adapted to that used in this chapter, is

$$\frac{x}{X_c} = \left(\frac{H(x)}{H_m}\right)^2 \left[3 - 2\left(\frac{H(x)}{H_m}\right)\right]. \tag{9.73}$$

This analytical solution was compared to observational data of the South Pass of the Mississippi river delta (Mississippi, USA), and to laboratory experiments, with the results found to be in close agreement (Fig. 9.3).

The non-dimensional salt-wedge configuration of the South Pass (Mississippi river) was also simulated by Wright (1970), using the Eq. (9.73) and the following quantities: $H_0 = 11.5$ m, $h_m = 7.3$ m and $H_m = 0.63$. Taking h = 0.0; 0.05; 0.1; 0.2; 0.3; 0.4; 0.5 and 0.6, the following values were obtained for the non-dimensional ratio $x/X_c = 0.0$; 0.02; 0.08; 0.27; 0.49; 0.70; 0.88 and 1.0, respectively. The results of the correlation, H/H_m, as a function of the non-dimensional distance, x/X_c, are shown comparatively in Fig. 9.3 (black points), and are almost coincident with the classical results of Farmer and Morgan (1953), with only a small deviation near the estuary mouth. In this figure, it is also possible

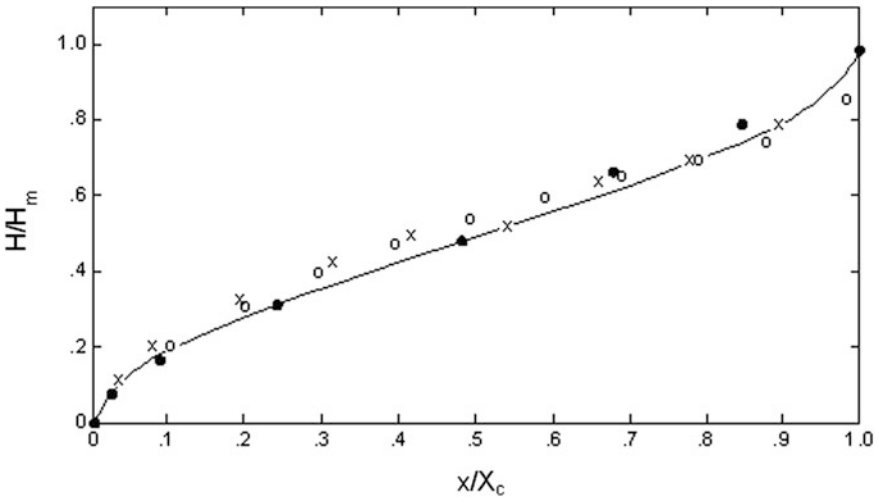

Fig. 9.3 Non-dimensional salt-wedge configuration. The continuous line is the theoretical result obtained with the Eq. (9.73). Observational data from the South Pass of the Mississippi river, and experimental laboratory data are indicated by o and x, respectively (according to Farmer and Morgan, 1953). Black points • were introduced to indicate theoretical results calculated with Equation (9.74)

to observe that for small values of the non-dimensional depth, that is, in the vicinity of the interior salt-wedge limit, the non-dimensional profile is approximately convex, gradually becoming linear in the medium portion of the wedge and, finally, slightly concave in the proximity of the estuary mouth.

This theoretical model has been generalized by Rattray and Mitsuda (1974) in order to include the bottom topography, with its declivity and the bottom friction. Also, in the theoretical development of the upper layer, a simplified equation of motion was used, which included the advective acceleration. To analytically formulate the motion in the lower layer (salt-wedge), several approximations from the classical articles also were used.

A theory of the density current in a stratified two-layer estuary flow with complete vertical mixing in the upper layer was developed by Prandle (1985). This theory was extended to the special case of a channel with a flat bed, constant breadth and depth. The theoretical result was further simplified, neglecting some undesirable effects, and an estimate of the salt-wedge intrusion length, L_{length}, was calculated by:

$$L_{length} = 0.26 \frac{gH_0^2}{ku\bar{u}} \frac{\Delta\rho}{\rho} = 0.26 \frac{g'H_0^2}{ku\bar{u}}. \tag{9.74a}$$

This result was compared with the following expression of the intrusion length, L_A, of an arrested salt wedge estuary given by G. H. Keulegan in 1949 (quoted in Ippen & Harleman, 1961), adding useful support to the above expression,

$$L_A = A \frac{g^{5/4} H_0^{9/4}}{\bar{u}^{5/2}} \left(\frac{\Delta\rho}{\rho}\right)^{3/4}. \tag{9.74b}$$

During the investigation of the dynamical interaction of the tidal flow with the estuarine circulation of the Fraser river salt wedge estuary, which has a characteristic two layer circulation, the *internal or densimetric Froude number*, G, (Chap. 2, Eq. 2.39), has been expressed by Geyer and Farmer (1989) as:

$$G^2 = (F_1)^2 + (F_2)^2, \tag{9.75}$$

where $(F_i)^2 = u_i^2/g'h_i$, (i = 1, 2), u_1 and u_2 are velocities in the upper and lower layers, respectively, g' is the reduced gravity, and h_1 and h_2 are the thicknesses of the upper and lower layers, respectively. For the simplified two-layer flow of a salt wedge estuary in a rectangular channel with a uniform depth-mean volume transport and a quasi-steady interface elevation, the momentum equations for the upper and lower layers where combined to form the following equation for density-driven shear flow (Geyer and Farmer, op. cit.):

$$\frac{\partial}{\partial t}(u_2 - u_1) = -[(1 - G^2)g' \frac{\partial \eta}{\partial x} + \frac{C_D |u_2| u_1}{h_2} + C_E(\frac{1}{h_1} + \frac{1}{h_2})|u_2 - u_1|(u_2 - u_1)]. \tag{9.76}$$

In this equation, $\eta = \eta(x)$ is the interface elevation, C_D and C_E are the bottom and interfacial drag coefficients, respectively; $C_E \ll C_D$ unless the interface is unstable. Since the interface slopes downward in the landward direction (Fig. 9.2), the first term on the right-hand-side of Eq. (9.76) will be positive or negative for subcritical and supercritical flows, respectively. The bottom drag term will be positive or negative, depending on the direction of the near-bottom flow. The magnitude of the interfacial drag term is difficult to ascertain, since it depends on the stability of the interface; however, its sign will always be such that it acts in opposition to the shear.

The solution of an *arrested salt wedge* is obtained when the left-hand-side of Eq. (9.76) vanishes and the baroclinic pressure gradient balances the drag terms. For this to occur, the flow must be subcritical, with the baroclinic pressure gradient balancing the drag of the landward deep flow.

Studies of the time dependent mixing in salt wedge estuary were presented by Partch and Smith (1978), analyzing measurements of salinity and velocity profiles, taken at short time intervals in comparison to the tidal period, as well as direct measurements of vertical turbulent salt flux and turbulent kinetic energy. Their results indicated that the turbulent mixing through the density interface is highly time dependent with the most intense mixing occurring at the maximum speed, and when the flow approaches critical conditions.

9.3 Theory and Experiment

Exemplifying the theory that has been developed, let us perform an analysis of the longitudinal salinity stratification presented in Fig. 9.1a. As previously indicated, this experimental result, which was observed during a period of high river discharge ($Q_f \approx 148\ m^3\ s^{-1}$) in the salt wedge estuary of the Duwamish river (Seattle, Washington, USA), was published by Dawson and Tilley (1972).

To adequate this experimental result to the presented theory, it is necessary to approximate the estuary with a simple geometry, for example: the bottom with a planel surface, with a mean depth of 10 m ($H_0 = 10$ m) and a constant width (B = 140 m, from hydrographic charts, Corps of Engineers 1973, quoted in Rattray and Mitsuda 1974). From Fig. 9.1a, it is possible to estimate the salt-wedge intrusion length as 10^4 m with a mean slope estimated as $d\eta_2/dx = 2.0 \times 10^{-4}$ (approximately 1.0 m for a length of 5000 m). The fresh water velocity at the estuary head is estimated as 0.10 ms^{-1}. Another quantity which may be estimated from the figure is the non-dimensional depth of the salt-wedge at the estuary mouth, calculated by the ratio $H_m = h_m/H_0 \approx 0.4$ ($h_m = 4$ m and $H_0 = 10.0$ m). With this

value, using Eq. (9.73), it is possible to calculate the non-dimensional configuration of the salt wedge, which is similar to that presented in Fig. 9.3.

These results show that it is possible to have good agreement between values obtained theoretically and experimentally, such as the salt-wedge intrusion length, using a determined value for the interfacial friction coefficient, k. However, this doesn't represent proof of the hypothesis used in the theory, because k is a measure of the eddy shear at the salt and fresh water interface, and its value varies not only with different estuary conditions, but also from one estuary to the other (Farmer and Morgan 1953; Rattray and Mitsuda 1974).

Let us continue to theoretically calculate the vertical velocity profile at the landward position, x≈7.8 km, in the salt wedge estuary (Fig. 9.1a). At this position, the thicknesses of the upper and lower layers during high river discharge are approximately h_1 = 4.0 m, h_2 = 6.0 m. Then, according to Eq. (9.10), the velocity in the upper layer (0 ≤ z ≤ 4 m) is calculated by

$$u_1(x) = u_f = \frac{Q_f}{Bh_1(x)} = 0.26\,\mathrm{ms}^{-1}.$$

The lower layer (salt-wedge) is delimited by the depth interval (4 m ≤ z 10 m), and the theoretical vertical velocity profile is calculated by Eq. (9.41). Using the values already determined for this profile, we have:

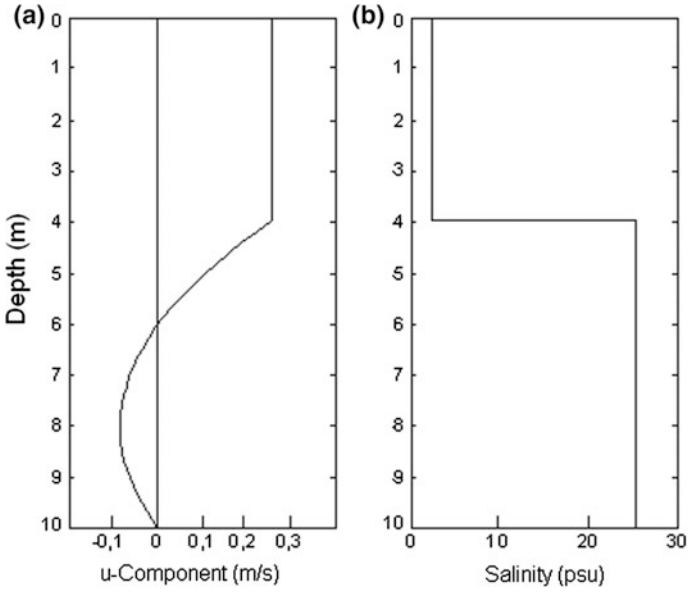

Fig. 9.4 **a** Theoretical vertical velocity profile in the salt wedge estuary of the Duwamish river. **b** Experimental vertical salinity profile. The physical quantities necessary to calculate these profiles were estimated from Fig. 9.1a

$$u_2(x,z) = -(\frac{0.52}{6})(10 - z) + (\frac{0.78}{36})(10 - z)^2,$$

or

$$u_2(x,z) = -8.7x10^{-2}(10 - z) + 2.2x10^{-2}(10 - z)^2.$$

Composing the profiles, $u_1(x)$ and $u_2(x, z)$, in the upper ($0 \leq z \leq 4$ m) and lower (10 m $\leq z \leq 4$ m) layers, we obtain the theoretical velocity profile in the water column, as shown in Fig. 9.4a; this solution is represented graphically, with the vertical salinity profile (Fig. 9.4b estimated from Fig. 9.1a. Figure 9.4a indicate that above the halocline, the flow is seaward with constant velocity, $u_1(x) = 0.26\,\mathrm{ms}^{-1}$. In the salt-wedge, an accentuated decrease is observed in the velocity, $u_2(x, z)$, and at 6 m depth the velocity is zero. For greater depths, the motion is landward and reaches a velocity of $-0.09\,\mathrm{ms}^{-1}$. At the depth interval of the salt-wedge the vertical velocity shear is forced by the barotropic pressure gradient and the free surface slope, and due to the imposed boundary condition the velocity at the bottom is zero.

As the theoretical velocity profile has been obtained with simplifying hypothesis, it must be validated by comparison with experimental velocity profiles.

References

Dawson, W. A. & Tilley, L. J. 1972. Measurement of Salt Wedge Excursion Distance in the Duwamish River Estuary, Seattle, Washington, by Means of the Dissolved-Oxygen Gradient. Geological Survey Water-Supply. Washington, D. C., U. S. Department of Interior, Paper 1873-D, pp. D1–D27.

Farmer, H. G. & Morgan, G. W. 1953. The Salt Wedge. In: Johnson, J. W. (ed.). Proc. of Third Conference on Coastal Engineering. Council on Wave Research. Cambridge, The Engineering Foundation, pp. 54–64.

Geyer, W. R. 1986. The Advance of a Salt Wedge Front: Observations and a Dynamical Model. In: Dronkers, J & Van Leussen W. (eds.). Physical Processes in Estuaries. Berlin, Springer-Verlag, pp. 181–195.

Geyer, W. R. & Farmer, D. M. 1989. Tide-Induced Variations of the Dynamics of a Salt Wedge Estuary. J. Phys. Oceanogr., v.19, pp.1060–1072.

Granville, W. A.; Smith, P. F. & Longley, W. R. 1956. Elementos de Cálculo Diferencial e Integral. Trad. J. Abdelhay. 2 ed., Rio de Janeiro, Editora Científica. 695 p.

Hansen, D. V. & Rattray Jr., M. 1966. New Dimensions in Estuary Classification. Limnol. Oceanogr., 11(3):319–325.

Harleman, D. R. F. & Ippen, A. T. 1967. Two-Dimensional Aspects of Salinity Intrusion in Estuaries: Analysis and Velocity Distributions. Committee on Tidal Hydraulics. Tech. Bull., Corps of Engineers, U. S. Army, n. 13.

Keulegan, G. H. 1949. Interfacial Instability and Mixing in Stratified Flows. J. Res. U. S. Geol. Surv., 43:487–500.

Officer, C. B. 1976. Physical Oceanography of Estuaries (and Associated Coastal Waters). New York, Wiley. 465 p.
Partch, E.N. & Smith, J.D. 1978, Time Dependent Mixing in a Salt Wedge Estuary. Estuarine and Coastal Marine Science. 6, pp. 3–19.
Prandle, D. 1985. On salinity Regimes and the Vertical Structure of Residual Flows in Narrow Tidal Estuaries. Estuar. Coast. Shelf Sci., 20:615–635.
Pritchard, D. W. 1955. Estuarine Circulation Patterns. Proc. Am. Soc. Civ. Eng., 81:717:1–11.
Rattray Jr., M. & Mitsuda, E. 1974. Theoretical Analysis of Conditions in a Salt Wedge. Estuar. Coast. Mar. Sci., 2:375–394.
Sanders, J. L.; Maximon, L. C. & Morgan, G. W. 1953. On the Stationary Salt Wedge – a Two Layer Free Surface Flow. Tech. Rept., Brown University, n. 1. 44 p.
Schettini, C. A. F. 2002. Caracterização Física do Estuário do Rio Itajaí-açu, SC. Revista Brasileira Recursos Hídricos, 7(1):123–142.
Schettini & Truccolo. E. C. 1999. Dinâmica da Intrusão Salina no Estuário do Rio Itajaí-açu. In: Congresso Latino Americano de Ciências do Mar, 8, Trujillo, Peru, Resumenes ampliados, Tomo II, UNT/ALICMAR, p. 639–640.
Shi-Igai, H. & Sawamoto, M. 1969. Experimental and Theoretical Modeling of Saline Wedges. Proc. of the 13th Congress Internat. Assoc. Hydraulic Res., Kyoto. Science Council of Japan, 3 (C): 29–36.
Wright, L. D. 1970. Circulation, Effluent Diffusion and Sediment Transport, Mouth of South Pass, Mississippi River Delta. Baton Rouge, Louisiana State University Press. 56 p.

Quoted References

Corps of Engineers. 1973 (quoted in Rattray & Mitsuda, 1974. Theoretical Analysis of Conditions in a Salt-Wedge. Estuar. Coast. Mar. Sci., 2:375–394).
Döbereiner, C.E. 1985. Comportamento hidráulico e sedimentológico do estuário do rio Itajaí, SC. Rio de Janeiro, Instituto Nacional de Pesquisas Hidroviárias (INPH), Relatório 700/03, 34 p. (quoted in Schettini (2002), p. 132).
Ippen, A. T. & Harleman, D. R. F. 1961. One-Dimensional Analysis of Salinity Intrusion in Estuaries. Committee on Tidal Hydraulics. Tech. Bull. Corps of Engineers U. S. Army, n. 5. 120 p.
Schijf, J.B. & Schonfeld, 1963. Theoretical considerations on the motion of salt and fresh water. Proc. Minnesota Int. Hydraul. Conv. 5th Congress I.A.H.R., pp. 321–333. (quoted in Geyer & Farmer (1989), p. 1060).